J. Geophys. 42, 705–716, 1977

Journal of Geophysics

# Interpretation of the Optical Properties of Interplanetary Dust

R. H. Giese

Bereich Extraterrestrische Physik, Ruhr-Universität Bochum,
Geb. NA 01/130, D-4630 Bochum, Federal Republic of Germany

**Abstract.** Recent micrometeorite flux curves and optical results about the radial distribution of interplanetary dust particles obtained by the Helios space probes provide valuable criteria for interpretation of zodiacal light measurements. It is shown, that models based on Mie-theory and small ($\lesssim 1\,\mu m$) particles are no longer consistent with observational results. The main contribution to zodiacal light seems to be based on larger ($>10\,\mu m$) particles. If polarization is taken into account, absorbing particles of fluffy structure must be adopted as an important component of the interplanetary dust cloud.

**Key words:** Zodiacal light – Interplanetary dust – Light scattering by small particles.

## 1. Introduction

The sun is surrounded by a thin dust cloud of particle number density $n(\bar{r})$ decreasing with increasing solar distance $r$. It is flattened and has its plane of symmetry (see Leinert et al., 1977) close but not exactly at the plane of the earth's orbit (ecliptic plane). Figure 1 illustrates roughly the shape (surfaces of equal $n$) of the cloud and the regions accessible by Helios ($H$) and by a possible out-of-ecliptic mission ($E$).

Solar light, scattered by interplanetary dust particles is observable as a component of the diffuse brightness of the night sky. It is also concentrated towards the ecliptic plane (zodiacal light), and decreases in intensity with increasing angle between the solar direction and the line of sight (elongation $\varepsilon$), except close to the antisolar direction ($160° \lesssim \varepsilon \lesssim 180°$), where a slight (ca. 30 %) increase of intensity is observed (Gegenschein). For small elongation the zodiacal light continuously merges into the dust component of the corona ($F$-corona).

Ground based observations and photometry from rockets and space vehicles have covered large regions of the sky including the ecliptic pole and small

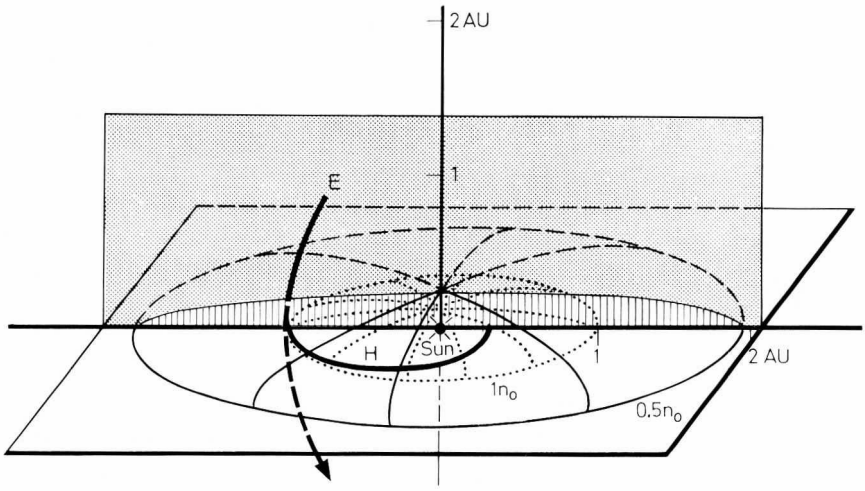


**Fig. 1.** Schematic view of the interplanetary dust cloud in the case of an ellipsoid model. The shape of the cloud (fan-like, ellipsoidal etc.) is still controversial (Fechtig et al., 1976; Dumont, 1976; Leinert et al., 1976). Distances in astronomical units, $1\,n_0$ and $0.5\,n_0$ surfaces of equal particle number density, *H* Helios orbit, *E* execliptic mission

elongations ($\varepsilon < 30°$). Latest results are reviewed by Leinert (1975), Dumont (1976), and Weinberg (1976).

Direct access to the interplanetary dust cloud has been possible by micrometeorite impact detectors on space vehicles (rockets, HEOS, Pioneer, Helios) and by analysis of microcraters on lunar samples. From these in situ records a rather reliable cumulative curve of interplanetary micrometeorite fluxes near 1 AU (astronomical unit) solar distance could be derived. Methods and results are reviewed by Fechtig (1976).

Interpretations of observational data, which were performed in connection with the Helios program proved the compatibility between the results of optical and of impact measurements. They suggest that the main contribution to the zodiacal light should be due to larger ($> 10\,\mu m$) particles of fluffy material. The arguments, which lead to this conclusion and the role Helios played in this field will be outlined in the following sections.

## 2. Problem and Definitions

For comparison with flux data obtained by impact detectors, the observations of zodiacal light need appropriate interpretation to convert brightness into number density and into properties of dust particles. The basic problem and its geometry is shown in Figure 2. If an observer $O_b$ at solar distance $a$ in the ecliptic plane looks in a given direction into a cone of the solid angle $d\Omega$, he receives scattered radiation from all dust particles in his viewing cone. The contribution of a volume element $dV$ on the line of sight to the surface brightness $I$ of the zodiacal

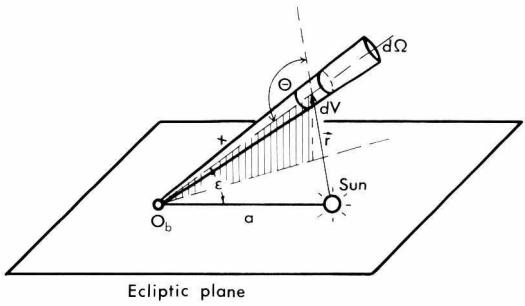


**Fig. 2.** Basic geometry for interpretation of the zodiacal light

light observed from $O_b$, is dependent on the illumination of $dV$, i.e. on the solar distance $r$, and on the local properties of the interplanetary dust cloud. These are

- the spatial distribution of the particle number density $n(\vec{r})$,
- the distribution function of particle sizes in the volume element $F(s)\,ds$,
- the properties of the individual particles (sizes, shape, material), represented by the light scattering function $\sigma(\theta, s, \lambda, m)$.

Here $m = m_1 - im_2$ is the complex refractive index (which depends on wavelength and material), $\theta$ the scattering angle (Fig. 2), $\lambda$ the wavelength, and $s$ the size (e.g. the radius) of the scattering particle. The absolute size can be substituted by a dimensionless size parameter $\alpha$, which is in the case of a spherical particle defined $\alpha = 2\pi s/\lambda$. For visible light ($\lambda = 0.5\,\mu m$) a particle of $\alpha = 10$ is $0.8\,\mu m$ in radius. The scattering function $\sigma(\alpha, m, \theta)$ is defined in this work as usual according to van de Hulst (1957). It has no dimension and is related to the differential scattering cross section (e.g. $[cm^2\,sr^{-1}]$) by the factor $\lambda^2/8\pi^2$. If the number density of particles contained in a volume is $n[cm^{-3}]$ a scattering function per unit of volume (volume scattering function, e.g. $[cm^2\,cm^{-3}\,sr^{-1}]$) can be defined as $\Sigma = (\lambda^2/8\pi^2)\,n\bar{\sigma}$.

For the surface brightness one obtains (Fig. 2)

$$I \sim \int_0^\infty \frac{n(\vec{r})\,\bar{\sigma}(\theta)\,dx}{r^2} \tag{1}$$

where

$$\bar{\sigma}(\theta) = \frac{\int_0^\infty \sigma(\theta, s, \lambda, m)\,F(s)\,ds}{\int_0^\infty F(s)\,ds} \tag{2}$$

is the average scattering function per one particle of the dust mixture within $dV$. For the purpose of this paper $\bar{\sigma}$ will be adopted as independent of location.

The problem can be treated separately for the component of the scattered light $I_\perp$ and $I_\parallel$ having the electric vector perpendicular and parallel to the plane

of vision (sun-particle-observer), respectively. Therefore it is also possible to derive the degree of linear polarization

$$P=\frac{I_{\perp}-I_{\parallel}}{I} \tag{3}$$

where $I=I_{\perp}+I_{\parallel}$. In a similar way linear polarization can be defined for scattering functions by $P=(\sigma_{\perp}-\sigma_{\parallel})/\sigma$, where $\sigma=\sigma_{\perp}+\sigma_{\parallel}$.

Observations can provide

- the surface brightness $I$
- the degree of polarization $P$
- the wavelength dependence of $I$ and $P$

as a function of the observer's position in the solar system and of the viewing direction. From these $n(\bar{r})$, $F(s)$ and $\sigma$ are to be derived.

Furthermore $\sigma(\theta, s, \lambda, m)$ has to be explained in terms of physical properties, such as material (absorbing, dielectric), shape (spherical, convex, lengthy, irregular), and structure (rough, fluffy, compact) of the dust particles.

Explicit formulae for (1) corresponding to different models of the three dimensional dust distribution (ellipsoidal, fan-like etc.) have been applied recently by Dumont (1975), Giese and Dziembowski (1969), Giese (1975), Fechtig et al. (1976), and Leinert et al. (1976). The following discussion, however, will be restricted to the dust distribution in the ecliptic plane. Further the well known approximation by a power law $n=n_0 r^{-\nu}$ will be used for the particle number distribution, where $n_0$ is number density of dust particles near the earth's orbit ($r$ in AU). In this case (1) yields after some geometric conversions

$$I(\varepsilon)\sim n_0(a\sin\varepsilon)^{-(\nu+1)}\int_{\varepsilon}^{\pi}\bar{\sigma}(\theta)(\sin\theta)^{\nu}\,d\theta. \tag{4}$$

## 3. Observational Material

Interpretations of the zodiacal light were suffering for a long time from large spread of observational data in both, photometric measurements and micrometeorite fluxes. Recent investigations have removed ambiguities and provided significant facts to be considered in any interpretation:

– The decrease of particle number densities with solar distance $r$ derived from zodiacal light measurements by space probes (Helios, Pioneer 10) can be approximated by $n(r)\sim r^{-\nu}$ with values of $\nu\simeq 1$ (Hanner et al., 1976) or $\nu\simeq 1.3$ (Link et al., 1976), which is in excellent agreement with the value of $\nu\simeq 1.2$ derived from ground based observations by Dumont and Sánchez (1975).

– Rather reliable volume scattering functions of the interplanetary dust were empirically derived from optical measurements (Dumont and Sánchez, 1975; Leinert et al., 1976).

– The spectrum of the zodiacal light is close to the solar spectrum not only in the visible range but up to infrared wavelength of some 2 μm (Nishimura, 1973; Frey et al., 1974).

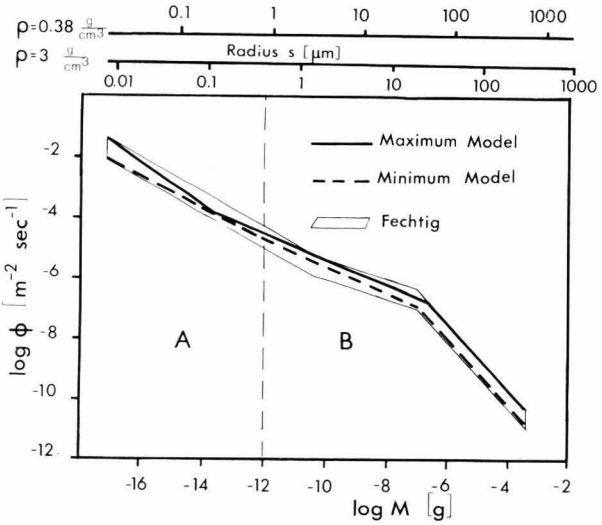


**Fig. 3.** Cumulative dust flux $\phi$ at $1\,AU$ (Fechtig, 1976). *A* relative velocity ca. 50 km/s from solar direction, *B* relative velocity ca. 10 km/s from earth apex, $M$ particle mass, $\rho$ density of particle material. Minimum and maximum model: Approximations for calculation of the brightness of the zodiacal light on the basis of the flux curve (Giese and Grün, 1976; Leinert et al., 1976)

– There is now a consistent curve (Fig. 3) for cumulative dust fluxes in interplanetary space near 1 AU (ref. Fechtig, 1976).

## 4. Interpretation

### *4.1. Empirical Scattering Functions*

Earlier interpretations of the zodiacal light were based on models fitted to the observed brightness $I(\varepsilon)$ by use of Equation (1). Since the integral implies both, number density and scattering properties, $n$ and $\sigma$ could not be derived independently.

It is a most important result of the Helios and Pioneer missions to show on a direct way, that the spatial density of interplanetary dust between 0.1 AU and 1.5 AU can be characterized by a value of $\nu$ between $\nu=1$ and $\nu=1.5$ if no spatial changes of the optical particle properties have to be taken into account. These results are based on the zodiacal light $I(\varepsilon_0, a)$ observed in a fixed looking direction ($\varepsilon_0=$const) while the space probe was changing its solar distance $a$. According to Equation (4) in this case the relative variation of brightness $I(\varepsilon_0) \sim a^{-(\nu+1)}$ is independent of $\bar{\sigma}(\theta)$. After $\nu$ is derived in this way it can be used independently to determine volume scattering functions $\Sigma(\theta)$ from observations of the run of $I(\varepsilon)$ with elongation. Empirical volume scattering functions as derived with $\nu=1$ by Leinert et al. (1976) and for $\nu=1.2$ by Dumont and Sánchez (1975) from terrestrial zodiacal light observations are combined in Figure 4A. Every dust mixture promising for interpretation of the zodiacal light

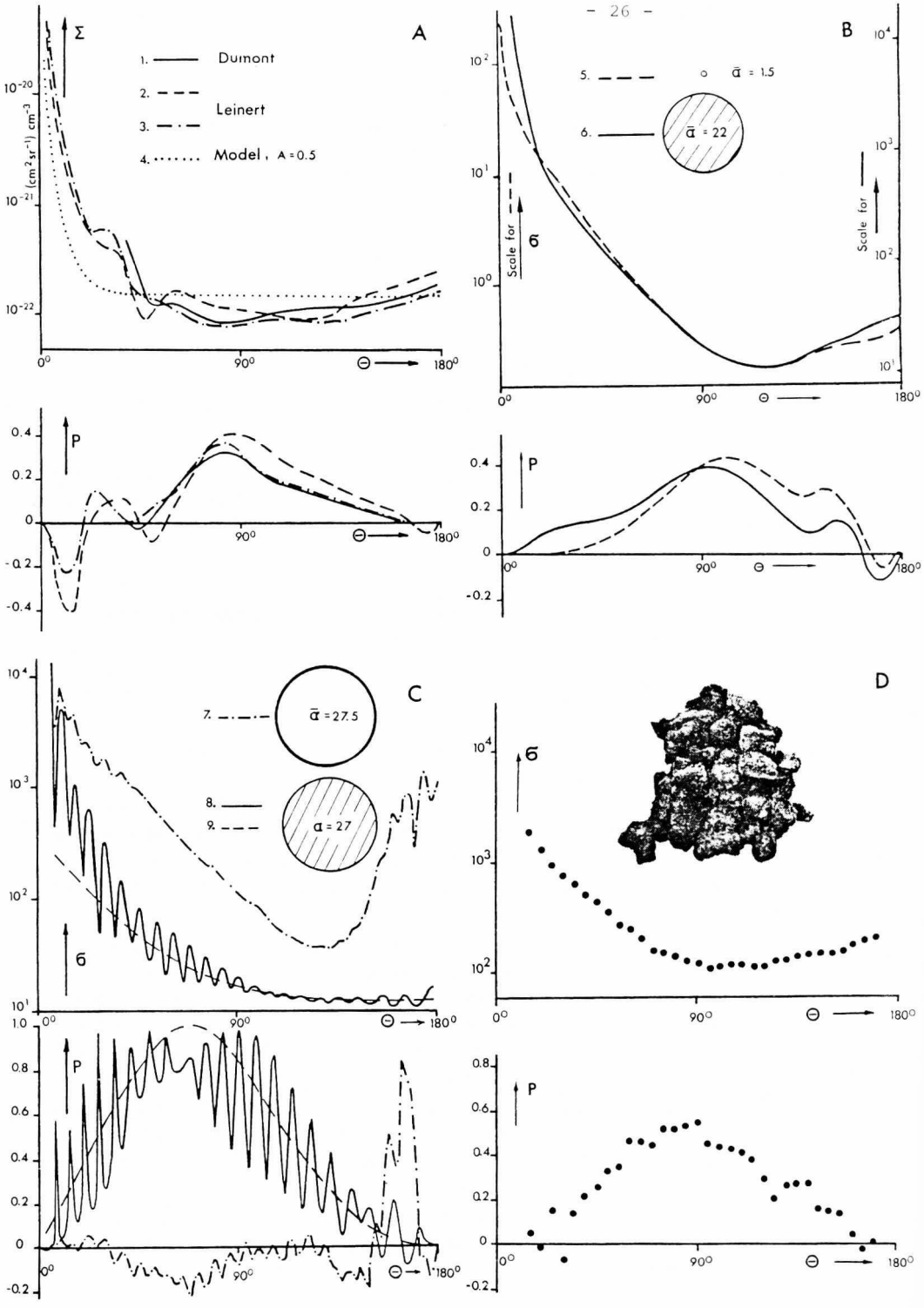
A
Σ
1. Dumont
2.
Leinert
3.
4. Model, A = 0.5
$10^{-20}$
$10^{-21}$
$10^{-22}$
$(cm^2 sr^{-1}) cm^{-3}$
0°
90°
Θ
180°
P
0.4
0.2
0
-0.2
-0.4
B
5. ō = 1.5
6. ō = 22
$10^2$
$10^1$
$10^0$
$10^4$
$10^3$
$10^2$
$10^1$
Scale for
б
Scale for
C
7. ō = 27.5
8.
9. ō = 27
$10^4$
$10^3$
$10^2$
$10^1$
1.0
0.8
0.6
0.4
0.2
0
-0.2
D
б
P

has to reproduce the essential properties of such empirical scattering functions: One feature is the rather isotropic behaviour of $\Sigma$ and therefore also of $\sigma(\theta)$ between $60° \lesssim \theta \lesssim 140°$. Outside this region $\sigma(\theta)$ rises by approximately a factor of 10 for forward scattering at $\theta \simeq 20°$ and in backward scattering region by about a factor of 2 towards $\theta = 180°$. Linear polarization $P(\theta)$ is positive in the region $60° \lesssim \theta \lesssim 170°$ with its maximum $P \simeq 0.3$ to 0.4 between $\theta = 80°$ to 90°. The region of negative polarization at $\theta \lesssim 50°$ will be excluded from discussion, since this region is considered as poorly reliable by Dumont and Sánchez (1975).

### *4.2. Models Based on Mie-Theory*

Interpretations of the zodiacal light were often based on the Mie-theory (see van de Hulst, 1957; Born and Wolff, 1965). They are restricted to the model of spherical particles but can take into account polarization and colour. The components necessary to approximate the observed polarization for $\varepsilon > 30°$ according to Mie-theory were either dielectric ($m = 1.33$) "submicron particles" of some tenth of a micrometer (Giese, 1962; Weinberg, 1964; Little et al., 1965) or absorbing particles of about half a micron in size (Giese and Dziembowski, 1969) or slightly absorbing particles in the micrometer range. Other possibilities were excluded by extensive survey calculations varying sizes and refractive indices (Giese, 1973). Leinert et al. (1976) with some reservations also used Mie-theory. They preferred larger ($> 1$ μm) and slightly absorbing particles to explain the polarization at low elongations ($\varepsilon \simeq 15°$) and the colour of the zodiacal light. But even these models, which are rather neutral in the colour dependence of scattered radiation (Giese et al., 1973) are based on a considerable percentage of particles in the size range below 10 μm.

In principle Mie-models are also appropriate to explain features like the Gegenschein (Walter, 1958) and the negative polarization observed in the region $170° \lesssim \varepsilon \lesssim 180°$ (Weinberg, 1964; Wolstencroft and Rose, 1967; Frey et al., 1974). This, however, could be attributed exclusively to a component of dielectric ($m_2 = 0$) or at most only slightly absorbing ($m_2 \lesssim 0.05$) particles since larger absorbing particles show positive polarization and a rather isotropic run of $\sigma(\theta)$ in the region of backward scattering (see 4.3).

**Fig. 4. A** Empirical volume scattering function $\Sigma(\theta)$ and polarization $P(\theta)$ of interplanetary dust. $\theta$ scattering angle (see Fig. 2), No. *1*. $\Sigma$ after Dumont and Sánchez (1975), No. *2* and No. *3*. $\Sigma$ after Leinert et al. (1976), No. *4*. Model calculation (diffraction plus isotropic reflection, albedo $A = 0.5$). **B** Scattering functions $\sigma$ and polarization $P$ of typical Mie-models. $m$ refractive index, $\alpha$ size parameter (= circumference/wavelength), size distribution $\sim \alpha^{-\kappa} d\alpha$, average size parameter $\bar{\alpha} = \int \alpha \cdot \alpha^{-\kappa} d\alpha / \int \alpha^{-\kappa} d\alpha$. No. *5*. mixture of dielectric submicron particles ($m = 1.33$, $\kappa = 4$, $1 \leqq \alpha \leqq 120$), No. *6*. mixture of slightly absorbing particles of micron size ($m = 1.33 - 0.01i$ and $m = 1.33 - 0.05i$; mixing ratio 1:2; $\kappa = 2.5$; $10 \leqq \alpha \leqq 120$). **C** Scattering functions $\sigma$ and polarization $P$ for larger spheres. No. *7*. mixture of dielectric spheres after Mie-theory ($m = 1.5$; $\kappa = 0$; $25 \leqq \alpha \leqq 30$), No. *8*. single absorbing sphere after Mie-theory ($m = 1.45 - 0.05i$; $\alpha = 27$). No. *9*. Same as No. 8, but Fresnelreflection. **D** Scattering function $\sigma$ and Polarization $P$ of a fluffy particle (*insert*). Average over many spatial orientations according to microwave measurements by Weiß (1977). $m = 1.45 - 0.05i$; $\alpha = 27$ ($\alpha$ for a sphere of same volume)

Figure 4B shows the average scattering functions ($\bar{\sigma}(\theta)$ and $P(\theta)$) of two typical Mie-models. The curves No. 5 correspond to a model of dielectric submicron particles ($\bar{x}=1.5$ or $\bar{s}\simeq 0.12\,\mu m$) having a steep size distribution ($\kappa=4$). If the run of $\bar{\sigma}(\theta)$ is adjusted to the volume scattering functions Figure 4A in the region $90°\lesssim\theta<180°$ the number density of such particles at 1 AU is found to be of the order $n_0\simeq 1\cdot 10^{-11}\,cm^{-3}$.

The other model (curve No. 6) presents the case of slightly absorbing particles with a flat size distribution ($\kappa=2.5$), mainly containing particles in the micrometer size range ($\bar{x}=22$, $\bar{s}\simeq 1.75\,\mu m$). The particle number density obtained for this type of models (curve No. 6) by comparing with Figure 4A is $n_0\simeq 2\cdot 10^{-13}\,cm^{-3}$.

If these number densities are converted into cumulative dust fluxes $\phi$ at 1 AU by assuming a relative velocity of 20 km/s, one arrives at $\phi\simeq 0.25$ for the model of curve No. 5 or $3.8\cdot 10^{-3}$ particles $m^{-2}\,s^{-1}$ for the model of curve No. 6, respectively. The corresponding masses of the smallest particles contained in the models are $M\simeq 6\cdot 10^{-15}$ or $6\cdot 10^{-12}$ g, if a density of $3\,g/cm^3$ is adopted for the material.

Before about 1970 there was no reason to reject such Mie-models, since there was a large divergence in cumulative flux values published on the basis of in situ measurements. For example, the cumulative flux at $M=6\cdot 10^{-12}$ g predicted by models like that presented in curve No. 6 was by a factor of $10^4$ too low compared to the compilation of particle fluxes presented in McCracken and Alexander (1965), but by more than a factor of 40 too high compared to the interplanetary flux model presented by McDonnell (1971).

For the spatial variation of $n(r)$ the Mie-models referred to above required values of $\nu\simeq 0$ to 0.5. This was due to the increase of the scattering functions to forward scattering, starting at scattering angles $\theta\lesssim 100°$. Therefore, to fit the observed increase of $I(\varepsilon)$ for decreasing elongation by use of Mie-scattering functions in Equation (4) it was not necessary to adopt any considerable increase of $n(r)$ towards the sun.

### *4.3. Consequences of Recent Results*

Further analysis of Helios data (Leinert et al., 1977) confirmed definitively the spatial dependence $n\sim r^{-\nu}$ with $\nu\simeq 1.3$. Furthermore the interplanetary flux curve seems now to be well represented by the rather narrow band given by Fechtig (1976) in Figure 3. Mie-models like in Figure 4B are not compatible with these results: They require $\nu\lesssim 0.5$; their scattering functions are not isotropic for $60°\lesssim\theta\lesssim 140°$; and the cumulative dust fluxes necessary to reproduce the zodiacal light are too high compared to Figure 3 (see 4.2).

To investigate in a more general way the compatibility between fluxes and zodiacal light data, Giese and Grün (1976) used the whole flux curve of Figure 3. They approximated $\phi(M)$ in different regions by appropriate power laws and converted them into differential size distributions by adopting $\rho=3\,g/cm^3$ for the particle density. The "Maximum Model" (Fig. 3) approximates the upper and the "Minimum Model" the lower limit of the fluxes. From this, $I(\varepsilon)$ was

computed according to Equation (4) with $\nu = 1$ and scattering functions which were constructed by diffraction plus isotropic reflection, allowing for an albedo $A$ (see Leinert, 1975). It turns out, that $I(\varepsilon)$ can be easily reproduced, except the rise towards the Gegenschein. With $A = 1$ the calculated intensity for example at $\varepsilon = 90°$ elongation is about twice the observed brightness for the Maximum Model or half the observed brightness for the Minimum Model, respectively. If instead of $\rho = 3\,\mathrm{g/cm^3}$ some fluffy material with $\rho = 0.38\,\mathrm{g/cm^3}$ were adopted, the particle diameters would be twice as large, which would result in an increase of the scattered intensity by a factor of 4. Therefore the particle number densities corresponding to $\phi(m)$ are completely sufficient to reproduce the observational brightness. One even can allow also for $A < 1$. Including the region of low elongations ($\varepsilon \lesssim 15°$) the Maximum Model with $A \simeq 0.5$ approximates the observations of $I(\varepsilon)$ and the volume scattering functions fairly well (see Fig. 4A; Leinert et al., 1976). When one separates the total brightness into contributions from different size intervals one sees that submicron particles and particles of only a few micrometers in size do not considerably contribute to the zodiacal light. For $\rho = 3\,\mathrm{g/cm^3}$ the contribution of particles with $s \lesssim 6\,\mu\mathrm{m}$ is only about 10%. The main contribution (70%) is due to particles in the size range between $s = 10$ to $80\,\mu\mathrm{m}$.

### 4.4. *Interpretation by Large and Fluffy Particles*

Approximations by diffraction and isotropic reflection have also been used for earlier interpretations of light scattering by interplanetary dust. Elsässer (1955), for example, derived from the brightness of the $F$-corona a flat run to the size distribution function ($\kappa \simeq 2$) and particle sizes in the region between 1 and $1000\,\mu\mathrm{m}$. In so far, his early results are in excellent agreement with the present view. On the other hand this and preceding models failed to explain polarization. They adopted as cause of polarization in the zodiacal light Thomson scattering by an extremely high number of electrons ($n_0 = 600$ electrons/$\mathrm{cm}^{-3}$; (Behr and Siedentopf, 1953), which later on turned out to be not realistic. Therefore it became necessary to base polarization on scattering properties of the dust particles. A first approach was to substitute Thomson scattering by scattering of small ($s \simeq 0.1\,\mu\mathrm{m}$) dielectric particles, which can produce polarization similar to Rayleigh scattering. Later models, such as No. 6 of Figure 4B, were proposed to avoid submicron particles and to obtain a flat ($\kappa = 2.5$) size distribution. All these models, which in principle were appropriate to reproduce polarization, at least for $\varepsilon > 30°$, must now be abandoned according to the arguments of Section 4.3. Therefore – as 20 years ago – there is again the problem of explaining polarization solely by scattering of larger ($\gtrsim 5\,\mu\mathrm{m}$) dust particles.

Dielectric spheres are not promising for this purpose. They produce, by no means, the isotropic scattering at medium scattering angles required by the empirical functions (Fig. 4A), but rather, show an increase with decreasing $\theta$ in the whole region of $\theta \lesssim 90°$ and an enhancement by more than one order of magnitude towards backward scattering. Polarization shows drastic positive peaks in the region of $130° \lesssim \theta \lesssim 180°$, completely inconsistent with Figure 4A.

These properties, demonstrated for spheres of $\bar{x} \simeq 27.5$ ($\bar{s} \simeq 2.2\,\mu m$) in Figure 4C (No. 7), have also been found for larger ($\alpha = 600$, $s = 48\,\mu m$) dielectric spheres (Hansen and Travis, 1974).

Effects like the strong peaks in the backward scattering region – for water droplets known as hazebow – are due to spherical geometry. They should not be present for mixtures of nonspherical, dielectric particles in random orientation. Indeed microwave analog measurements simulating mixtures of practically dielectric ($m = 1.57 - 0.006\,i$) cubes and octahedrons corresponding to particles in the micrometer size range showed rather neutral polarization and approximately isotropic scattering – in contrast to spherical particles (Zerull, 1976). Dielectric particles of nonspherical shape in random orientation may therefore be a component of interplanetary dust, which helps to lower strong polarization produced by other scattering processes, but they are not appropriate to explain the positive polarization of the empirical volume scattering functions.

Large absorbing spheres show mainly Fresnel-reflection outside the diffraction region, since most of the refracted radiation is absorbed inside the particle. In this case polarization is positive (Fig. 4C, No. 8), but with the maximum much stronger and at lower scattering angles than in the empirical curves. Only for rather unusual indices of refraction (like $m = 0.3 - 0.6\,i$) the position of the maximum (Brewster angle) can be shifted towards $\theta \simeq 90°$ (Matsumoto, 1973). Furthermore $\sigma(\theta)$ does not show an enhancement towards backward scattering like the scattering functions of Figure 4A.

Large absorbing nonspherical particles in random orientation having smooth and convex surfaces should show the same properties outside the diffraction region if only reflection at the surface has to be considered (van de Hulst, 1957). Zerull (1976) and Weiß (1977) proved by microwave analog measurements even in the size range $10 \lesssim \alpha \lesssim 30$ with $m = 1.45 - 0.05\,i$ and $1.65 - 0.25\,i$ that for absorbing compact bodies of irregular shape polarization is positive and close to Fresnel-reflection, i.e. the maximum is too strong and at a lower scattering angle than in Figure 4A. There still remains the problem to explain the correct run of polarization.

The solution may be found in the existence of fluffy particles (conglomerates of smaller particles) as shown by the insert of Figure 4D. If such particles are absorbing, they can produce at the same time a rather isotropic run of $\sigma(\theta)$ for medium scattering angles, slightly enhanced backward scattering approximately in agreement with Figure 4A, and positive polarization close towards the position of the maximum polarization in the empirical volume scattering function derived from the zodiacal light. Figure 4D shows an example obtained by microwave measurements (Weiß, 1977). Generally such measurements suggest that the maximum of positive polarization decreases in magnitude and is shifted towards $\theta = 90°$ the more the particle structure is fluffy, i.e. the more it deviates from a compact and smooth surface (Zerull, 1976). The same tendency was found for the dependence of polarization on the surface of lunar samples (Dollfus et al., 1971).

A theoretical model is presented by Wolff (1975). He explains by superposition of single and double Fresnel reflection and by shadowing effects features like the shift in the position of the maximum of positive polarization

and the enhanced backward scattering. Even the negative polarization observed in the photometric curves of the moon and minor planets at large scattering angles is explained. This could also be interesting for interpretation of the negative polarization of the zodiacal light without dielectric particles.

However Wolff's model is based on Fresnel reflection on facets, i.e. on geometric optics. On the other hand the microwave measurements were done with scattering objects of only some wavelengths in size ($\alpha \lesssim 30$). The fact, that in both cases similar effects were found suggests, that the scattering properties referred to above are rather independent of size and typical for particles having a fluffy surface microstructure.

These aspects are very fortunate for interpretations of the zodiacal light. They suggest that the scattering properties of interplanetary dust grains causing the zodiacal light can be explained rather unconstrained by very rough or fluffy, absorbing particles in the size range of some microns to even some hundred of microns, i.e. by a type of particle which is also suggested by meteors and by samples of interplanetary particles captured in experiments with high flying aeroplanes and rockets. A similar model for zodiacal light particles is also proposed by Hayakawa et al. (1975) on the basis of results concerning light scattering by cometary dust. It is quite possible that detailed models based on components of absorbing and fluffy particles are quite appropriate to explain the complete run of $I(\varepsilon)$ from the corona to the Gegenschein, polarization including negative polarization at high elongations, and colour of the zodiacal light. This statement, however, has to be still corroborated by further laboratory experiments on rough and fluffy particles including sizes from 10 to some 100 μm and by model calculations which cover a much larger range of parameters than the few special examples referred to in this work.

*Acknowledgements.* I wish to thank Drs. R. Dumont, E. Grün, M. Hanner, C. Leinert, R. Zerull, and Dipl.-Phys. G. Schwehm for useful discussions. This work was in part supported by the Bundesministerium für Forschung und Technologie via DFVLR-BPT contract WRS 0108.

## References

Behr, A., Siedentopf, H.: Untersuchungen über Zodiakallicht und Gegenschein nach Lichtelektrischen Messungen auf dem Jungfraujoch. Z. Astrophys. **32**, 19–50, 1953

Born, M., Wolf, E.: Principles of optics, 3rd ed. Oxford: Pergamon Press 1965

McCracken, C. W., Alexander, W. M.: Interplanetary dust particles. In: Introduction to space science (M. N. Hess ed.), pp. 423–472. New York-London-Paris: Gordon and Breach 1965

Dollfus, A., Geake, J. E., Titulaer, C.: Polarimetric and photometric properties of Apollo lunar samples. Summary of the report presented at the Lunar Science Conference Houston (Texas), Observatoire de Paris-Meudon, 1971

Dumont, R., Sánchez, F.: Zodiacal light photopolarimetry. II. Gradients along the ecliptic and phase functions of interplanetary matter. Astron. & Astrophys. **38**, 405–412, 1975

Dumont, R.: Ground-based observations of the zodiacal light. In: Lecture notes in physics, Vol. 48 (Interplanetary dust and zodiacal light) (H. Elsässer, H. Fechtig, eds.), pp. 85–100. Berlin-Heidelberg-New York: Springer 1976

Elsässer, H.: Fraunhofer-Korona und Zodiakallicht. Z. Astrophys. **37**, 114–124, 1955

Fechtig, H.: In-situ records of interplanetary dust particles – Methods and results. In: Lecture notes in physics, Vol. 48 (H. Elsässer, H. Fechtig, eds.), pp. 143–158. Berlin-Heidelberg-New York: Springer 1976

Fechtig, H., Giese, R. H., Hanner, M. S., Zook, H. A.: Investigation of interplanetary Dust from Out-

of-Ecliptic Space Probes. In: GSFC-X-660-76-53 Proc. of the Symposium on the Study of the Sun and Interplanetary Medium in Three Dimensions (L. A. Fisk, W. I. Axford, eds.), pp. 298–320. Greenbelt, Md.: Goddard Space Flight Center Technical Information Division 1976

Frey, A., Hofmann, W., Lemke, D., Thum, C.: Photometry of the zodiacal light with the balloon-borne telescope THISBE. Astron. & Astrophys. **36**, 447–454, 1974

Giese, R. H.: Light scattering by small particles and models of interplanetary matter derived from the zodiacal light. Space Sci. Rev. **1**, 589–611, 1962

Giese, R. H.: Optical properties of single-component zodiacal light models. Planet. Space Sci. **21**, 513–521, 1973

Giese, R. H.: Out-of-ecliptic dust. Eldo-Cecles/Esro-Cers Scient. and Tech. Rev. **7**, 43–51, 1975

Giese, R. H., Dziembowski, v., C.: Suggested zodiacal light measurements from space probes. Planet. Space Sci. **17**, 949–956, 1969

Giese, R. H., Grün, E.: The compatibility of recent micrometeoroid flux curves with observations and models of the zodiacal light. In: Lecture notes in physics, Vol. 48 (H. Elsässer, H. Fechtig, eds.), pp. 135–139. Berlin-Heidelberg-New York: Springer 1976

Giese, R. H., Hanner, M. S., Leinert, C.: Color-dependence of zodiacal light models. Planet. Space Sci. **21**, 2061–2072, 1973

Hanner, M. S., Sparrow, I. G., Weinberg, J. L., Beeson, D. E.: Pioneer 10 observations of the zodiacal light brightness near the ecliptic: Changes with heliocentric distance. In: Lecture notes in physics, Vol. 48 (H. Elsässer, H. Fechtig, eds.), pp. 29–35. Berlin-Heidelberg-New York: Springer 1976

Hayakawa, S., Matsumoto, T., Ono, T.: Optical properties of cometary dust. In: Lecture notes in physics, Vol. 48 (H. Elsässer, H. Fechtig, eds.), pp. 323–327. Berlin-Heidelberg-New York: Springer 1976

Hansen, J.E., Travis, L.D.: Light scattering in planetary atmospheres. Space Sci. Rev. **16**, 527–610, 1974

van de Hulst, H.C.: Light scattering by small particles. New York: Wiley 1957

Leinert, C.: Zodiacal light – A measure of the interplanetary environment. Space Sci. Rev. **18**, 281 – 339, 1975

Leinert, C., Link, H., Pitz, E., Giese, R.H.: Interpretation of a rocket photometry of the inner zodiacal light. Astron. & Astrophys. **47**, 221–230, 1976

Leinert, C., Pitz, E., Hanner, M., Link, H.: Observations of the zodiacal light from Helios 1 and 2. J. Geophys. **42**, 699 – 704, 1977

Link, H., Leinert, C., Pitz, E., Salm, N.: Preliminary results of the Helios A zodiacal light experiment. In: Lecture notes in physics, Vol. 48 (H. Elsässer, H. Fechtig, eds.), pp. 24–28. Berlin-Heidelberg-New York: Springer 1976

Little, S.J., O'Mara, B.J., Aller, L.H.: Light scattering by small particles in the zodiacal cloud. Astronomical J. **70**, 346–352, 1965

Matsumoto, T.: On the origin of the zodiacal light. Publ. Astron. Soc. Japan **25**, 469–480, 1973

McDonnell, J.A.M.: Review of in situ measurements of cosmic dust particles. Space Research XI, pp. 415–435. Berlin: Akademie-Verlag 1971

Nishimura, T.: Infrared spectrum of zodiacal light. Publ. Astron. Soc. Japan **25**, 375–384, 1973

Walter, H.: Theoretische Deutung des Gegenscheins durch Lichtstreuung an sphärischen Partikeln. Z. Astrophys. **46**, 9–16, 1958

Weinberg, J.L.: The zodiacal light at 5300 Å. Ann. Astrophys. **27**, 718–738, 1964

Weinberg, J.L.: Space observations of the zodiacal light. In: Lecture notes in physics, Vol. 48 (H. Elsässer, H. Fechtig, eds.), pp. 3–18. Berlin-Heidelberg-New York: Springer 1976

Weiß, K.: Untersuchung des Streuverhaltens von unregelmäßig geformten, absorbierenden Partikeln mit Mikrowellen. Diplomarbeit, Bereich Extraterrestrische Physik, Ruhr-Universität Bochum 1977

Wolff, M.: Polarization of light reflected from rough planetary surface. Applied Optics **14**, 1395–1405, 1975

Wolstencroft, R.D., Rose, L.J.: Observation of the zodiacal light from a sounding rocket. Astronomical J. **147**, 221–292, 1967

Zerull, R.H.: Scattering measurements of dielectric and absorbing nonsherical particles. Beitr. Phys. Atmosph. **49**, 168–188, 1976

*Received February 16, 1977; Revised Version March 18, 1977*